

Shock Scaffolds for 3D Shapes in Medical Applications

Frederic F. Leymarie and Benjamin B. Kimia, Brown University, RI, USA

Extended abstract — February 1st, 2003 — DIMACS Workshop

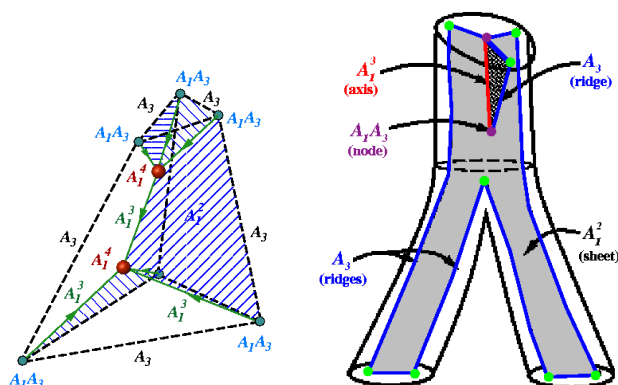


Figure 1: Illustration of the 3D augmented shock scaffold, SC^+ . The dark broken lines are in correspondence to surface ridges (A_3), while the smaller dots correspond to surface vertices (A_1A_3). The larger nodes are A_1^4 shocks, the interior links have arrows to indicate flow (all A_1^3 's here), the hashed sheets are hyperlinks (A_1^2 ; not all shown). *Left:* The SC^+ for a truncated tetrahedron consists of 8 nodes, 7 links and 9 hyperlinks. *Right:* Sketch of the SC^+ for a branching structure which at the top is a cylinder whose base grows from a triangle to an ellipse, and which splits into two cylindrical structures with elliptic bases (only the hyperlink interior to the shape is shown).

The shock scaffold is a hierarchical organization of the medial axis (\mathcal{MA}) in 3D consisting of special medial points, and curves connecting these points, thereby forming a geometric directed graph [5] (Fig.1). We will describe a new method for computing the shock scaffold for an unorganized cloud of points in 3D,¹ *e.g.*, as obtained from Computerized Tomography (CT) scanners (Fig.2), and illustrate some potential medical applications. Our method addresses the requirement of computing the \mathcal{MA} of realistic datasets, which involve tens or hundreds of thousands of points, in a practical time-frame (seconds). Our approach is based on propagation along the scaffold from initial sources of flow as a means to efficiently construct it. The detection of these sources can be shown to be

¹We join to this abstract a refereed conference paper under consideration, which summarizes the computational aspects of our new method.

reduced to considering pairs of input points, which then constitutes the computational bottleneck of this method [5]. We present seven geometric principles which avoid the consideration of those pairs of points which cannot possibly lead to a shock flow. Specifically, these steps involve (i) the “visibility” of a point from another, (ii) the clustering of points, (iii) the visibility of a cluster from another, (iv) the convex hull of a cluster, (v) the vertices of such convex hulls as “virtual” points, (vi) a multi-resolution framework, and, finally, (vii) a search strategy organized in layers.

In medical imaging and biology, the \mathcal{MA} is being used in a growing number of applications, including the characterization of the morphometry of bones [16], the registration of CT and Magnetic Resonance (MR) datasets [11, 10], anatomical model matching [17], path planning for virtual endoscopy [20, 12], the tracking of live cell pseudopode dynamics [9], the study of growth and morphogenesis [3], the study of 3D distribution of chromosomes [15]. Medial representations based on the \mathcal{MA} to model boundaries in 2D and 3D medical images is being explored, for example by Pizer *et al.* [14, 19]. Such medial structures are found helpful in image segmentation tasks to drive deformable templates permitting to characterize anisotropic growth mechanisms [13]. In computational chemistry and molecular design the \mathcal{MA} is used to skeletonize electron density maps to help automate the tracing of the molecular chains linking different atomic centers [6]. In drug design, the \mathcal{MA} should be a suitable substrate for building molecular surfaces and volumes [2], modeling receptor sites, the docking of ligands inside protein cavities [7], the contracting geometric invariance among molecules exhibiting similar activity, all key geometric problems in this field [4].

While most other approaches only approximate the 3D \mathcal{MA} , our approach based on the shock scaffold is exact. Furthermore, the algorithmic method based on the above computational geometry principles leads to quasi-linear numerical complexity in the computation of full scaffolds (Fig.2.(e)). This method presents an alternative to the classical approaches based on computing Voronoi diagrams (\mathcal{VD}), *e.g.*, via the QHULL algorithm [1]. Our timings are in the same ballpark as those based on QHULL for comput-

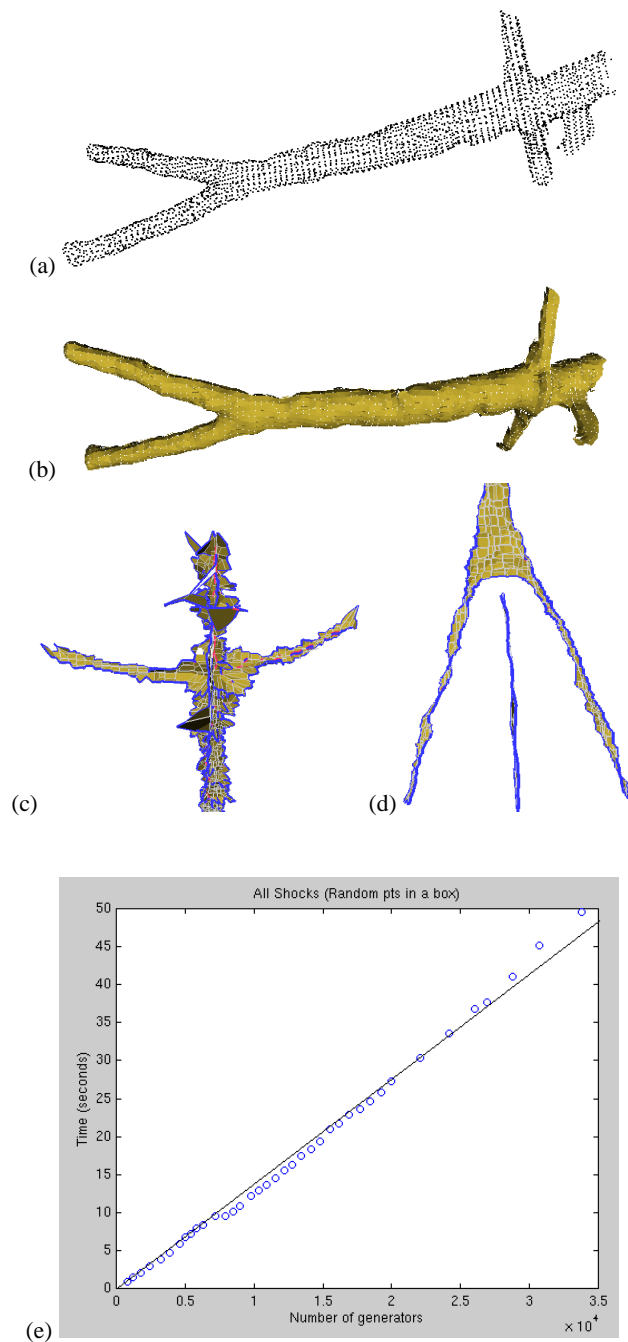


Figure 2: (a) 7691 point generators obtained from a CT scan of a human aorta [18]. (b) Automatic surface recovery \hat{S} derived from the shock scaffold SC [5], where white dots indicate generators. (c) SC^+ for the top interior part of the aorta, and (d) for the bottom interior and exterior part. Blue curves represent A_3 ribs, while pink curves represent A_1^3 axial curves. (e) Timing results for the shock flow method on a set of artificially generated random samples in a 3D box; experiments performed on an SGI Octane 2 machine running IRIX 6.5.

ing \mathcal{VD} , but the latter have theoretical problems in converging to the \mathcal{MA} [1, 5] and compute less structure. Note also that our method for computing the shock scaffold to represent the 3D \mathcal{MA} provides a new alternative to compute the \mathcal{VD} , with a number of interesting features including the locality of computations, and the ability to deal with dynamic inclusions and coarse-to-fine strategies.

Our presentation consists of three main parts. (i) We summarize the definition of the shock scaffold hierarchy, which is based on the notion of contact with maximal spheres and singularities of shock flows [8], and explain its relation to the \mathcal{MA} and \mathcal{VD} . (ii) We present the main aspects of our new method to compute the shock scaffold of unorganized points clouds in 3D [5]. (iii) We illustrate a number of potential applications in the medical and related fields, including the modeling of human body and tissue structures.

References

- [1] N. Amenta et al. A new Voronoi-based surface reconstruction algorithm. *Computer Graphics (SIGGRAPH'98)*.
- [2] M. Chapman and M. Connolly. *Molecular Surfaces*. International Tables for Crystallography (F). 2001.
- [3] S. Czanner et al. Growth simulation of human embryo brain. In *IEEE 17th Spring Conf. on Comp. Graphics*, 2001.
- [4] P. Finn and L. Kavraki. Computational approaches to drug design. *Algorithmica*, 25:347–371, 1999.
- [5] F. Føl-Leymarie. *Three-Dimensional Shape Representation via Shock Flows*. PhD thesis, Brown University, May 2003.
- [6] T. Ioerger and J. Sacchettini. Automatic modeling of protein backbones. *Acta Crystallographica*, D58(12), 2002.
- [7] R. Lewis and S. Bridgett. Conic tangency equations and Apollonius problems. *Maths. Comp. in Simul.*, 61(2), 2003.
- [8] F. Leymarie and B. Kimia. The shock scaffold for representing 3D shape. Springer, LNCS 2059:216–229, 2001.
- [9] F. Leymarie and M. Levine. Tracking deformable objects. *IEEE Trans. on PAMI*, 15(6):617–634, 1993.
- [10] A. Liu et al. 3D/2D registration via skeletal near projective invariance in tubular objects. In *MICCAI'98*.
- [11] M. Näf et al. 3D Voronoi skeletons. *CVIU*, 66(2), 1997.
- [12] D. Paik et al. Automated flight path planning for virtual endoscopy. *Medical Physics*, 25(5):629–637, 1998.
- [13] S. Pizer et al. Segmentation, registration, and measurement of shape variation. *IEEE Trans. Med. Ima.*, 18, 1999.
- [14] S. Pizer et al. Object models in multiscale intrinsic coordinates via m -reps. *IVC*, 21(1):5–15, 2003.
- [15] H. Scherthan et al. Aspects of three-dimensional chromosome reorganization. *J. Cell Science*, 111(16), 1998.
- [16] T. Sebastian et al. Segmentation of carpal bones from 3D CT images. In *MICCAI*, pages 1184–1194, 1998.
- [17] G. Székely. *Shape Characterization by Local Symmetries*. Habilitationsschrift, ETH Zurich, Switzerland, 1996.
- [18] A. Verroust and F. Lazarus. Extracting skeletal curves from 3D scattered data. *Visual Computer*, 16(1):15–25, 2000.
- [19] P. Yushkevich et al. Continuous medial representations for geometric object modeling in 2D and 3D. *IVC*, 21(1), 2003.
- [20] Y. Zhou et al. Three-dimensional skeleton and centerline generation. *Visual Computer*, 14(7):303–314, 1998.